Mechanical Design and Structural Analysis for Lower Port Optics of ITER Divertor Impurity Monitor*)

Toshiyuki MARUYAMA, Toshihiro OIKAWA[1)], Sin-iti KITAZAWA[1)], Kimihiro IOKI, Saori MERA, Ikuma NOMURA, Hiroaki OGAWA[1)], Suguru TANAKA[1)] and Takaki HATAE[1)]

TOYAMA Co. Ltd., Yamakita-machi, Ashigarakami-gun, Kanagawa 258-0112, Japan

[1)]*Naka Fusion Institute, National Institutes for Quantum and Radiological Science and Technology, Naka, Ibaraki 311-0193, Japan*

(Received 4 January 2019 / Accepted 17 March 2019)

The Divertor Impurity Monitor (DIM) for ITER is a spectroscopic diagnostic that measures the parameters of impurities and isotopes of hydrogen in the divertor plasmas. The DIM systems are installed in upper port, equatorial port, lower port (LP) and the divertor cassette. The LP systems consist of the side-upper/lower optical systems and the central optical system. In the central system, the front-end optics (optical mirrors) are located under the divertor-dome and this optics is required to have a structure that can withstand extremely high thermal loads in terms of establishing a sensitive optical structure. This paper presents a mechanical design of the optics with taking manufacturability into account and structural integrity assessment according to ITER load conditions (thermal and electro-magnetic loads, etc.) and design criteria specified in the RCC-MR code. The mechanical design of the optics forms a box-shaped optics and the structural analysis results indicate the mirror box satisfies design criteria in the RCC-MR code, except for the inner support part interfacing with the divertor cassette.

Keywords: ITER, plasma diagnostics, lower port, divertor cassette, structural analysis

DOI: 10.1585/pfr.14.3405080

1. Introduction

The main function of the ITER Divertor Impurity Monitor (DIM) is to measure the parameters of impurities and isotopes of hydrogen (tritium, deuterium and hydrogen) in the divertor plasmas by using spectroscopic techniques in the wavelength range of 200 - 1000 nm [1, 2]. Japan Domestic Agency is responsible for procurement of the DIM system. The DIM consists of five optical systems, one system in upper port, one system in equatorial port and three systems in lower port (LP). The DIM in LP consists of the side-upper and side-lower optical systems, which view through the gap of the divertor cassettes respectively from the upper side and the lower side of the LP, and the central optical system, which directly measures the inner and outer vertical targets of the divertor cassette as shown in Fig. 1. In the central optical system, the front-end optics (optical mirrors) are located under the divertor-dome and this optics is required to have a structure that can withstand extremely high thermal loads, in terms of establishing a sensitive optical structure such that precise optical mirrors are installed in the limited space, and the loads in the divertor area are much higher than in the vacuum vessel port (upper, equatorial and lower ports) area where other optical diagnostic systems are normally located. In the previous work [3], the thermal structure of a box-shaped optics, named mirror box, on the divertor cassette was developed and its structural feasibility against high thermal loads was

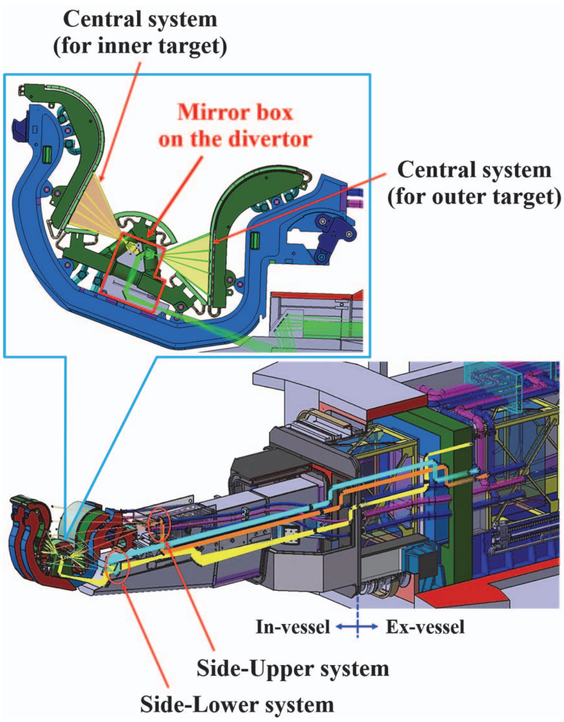

Fig. 1 DIM optical systems in LP.

author's e-mail: t-maruyama@toyama-jp.com

*) This article is based on the presentation at the 27th International Toki Conference (ITC27) & the 13th Asia Pacific Plasma Theory Conference (APPTC2018).

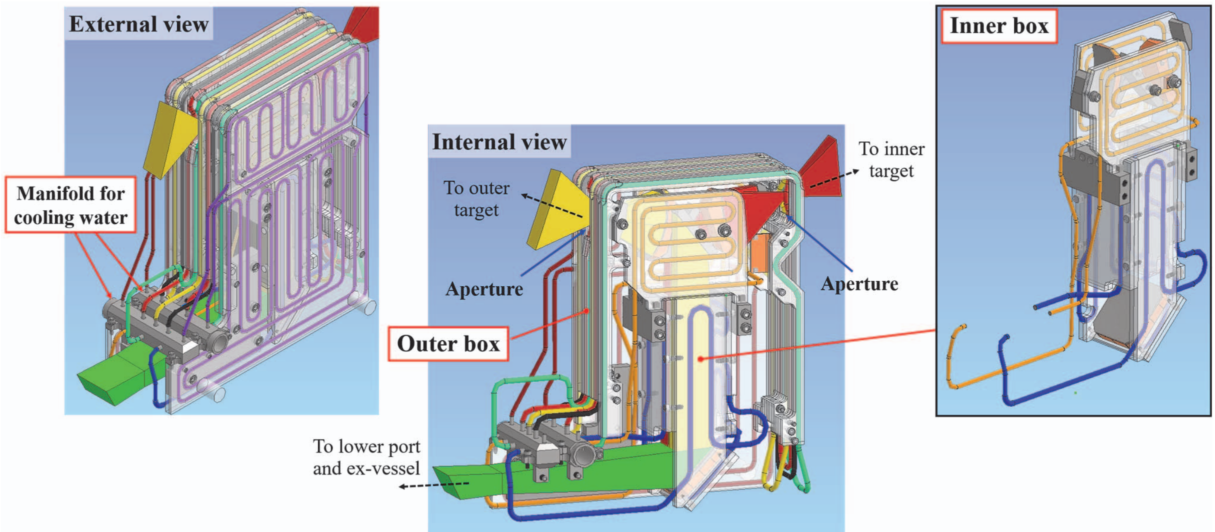

Fig. 2 Mechanical design of mirror box.

investigated. However, other mechanical loads (electromagnetic and seismic loads, etc.) and manufacturability of the mirror box were not taken into account. In this paper, a mechanical design of the optics with taking manufacturability into account was developed and its structural integrity assessment according to ITER load conditions and design criteria specified in the RCC-MR code [4], which was developed for sodium-cooled fast reactors and ITER Vacuum Vessel, was carried out.

2. Mechanical Design of Mirror Box on the Divertor Cassette

The detailed mechanical design of the mirror box on the divertor cassette was developed with taking into account manufacturability and actual assembly. The design and optical paths and mirrors in the mirror box are shown in Figs. 2 and 3. The mirror box consists of two-boxes structure, inner and outer boxes, for assembly and adjustment of optical mirrors. The main function of the inner box is to support the mirrors and of the outer box is to protect the mirrors against radiative plasma heat loads and dusts. A cooling pipe is embedded inside the plate of the mirror box.

Materials of the mirror box are stainless steel, SS316L, and copper. Copper is partially used to reduce temperature and thermal stress due to high thermal loads. The mirrors are attached on the plate with cooling circuit, cooling paths are not embedded in the mirrors themselves. A high temperature gradient occurs on the 1st and 4th mirrors due to high thermal loads for 1st mirrors and mirror size for 4th mirror, so that these mirrors consist of mirror surface made of SS316L, 3 mm thickness, and mirror base made of copper in order to improve thermal conduction as shown in Figs. 4 (a) and (b). The SS316L mirror surface and the copper mirror base are joined by explosive

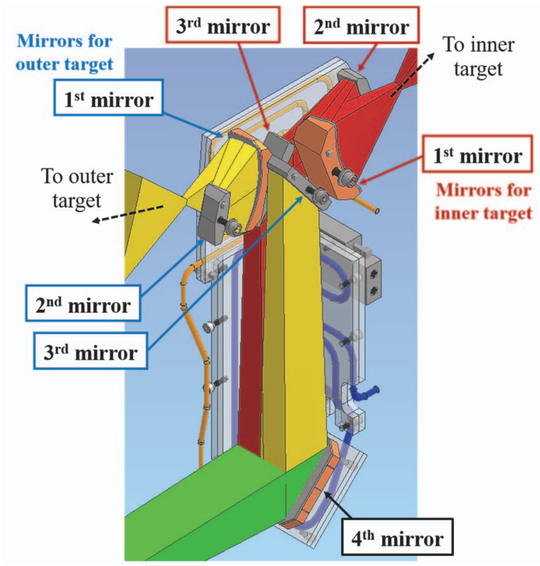

Fig. 3 Optical paths and mirrors in the mirror box.

bonding. An effective material for reflectivity in ultraviolet region (molybdenum, rhodium etc. to be determined) is coated on all mirror surfaces, 1st to 4th mirrors. An additional improvement of thermal conduction for 1st mirrors is required due to high thermal loads, so that a copper alloy block is embedded in the part of the inner box plate which contacts with 1st mirror as shown in Fig. 4 (c).

A concept of manufacturing and mechanical design of a plate with a cooling pipe is shown in Fig. 5. The plate with a cooling pipe is manufactured so that a bent pipe is sandwiched between plates channeled along the piping and joined by HIP (Hot Isostatic Pressing). The outer box forms a cooling water circuit with narrow gaps between cooling paths as possible in order to withstand extremely high radiative plasma heating, which are much higher than in the vacuum vessel port area where other optical diagnos-

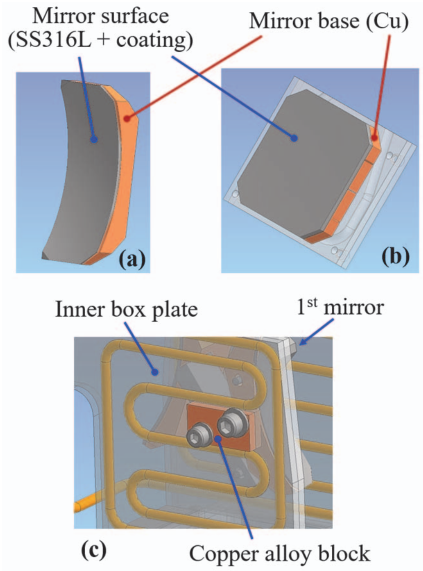

Fig. 4 Parts with improved thermal conduction; (a) 1st mirror, (b) 4th mirror and (c) inner box plate in contact with 1st mirror.

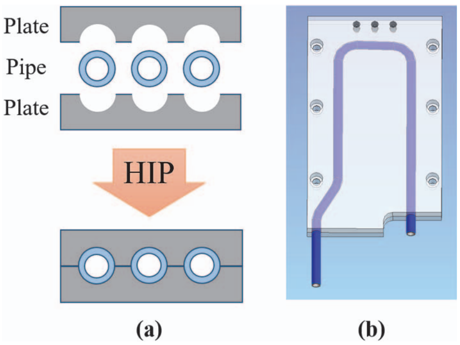

Fig. 5 Box plate with cooling pipes; (a) concept of manufacturing and (b) mechanical design.

tic systems are normally located. Since the plasma facing sides directly receive radiative plasma heating, the plates on the plasma sides require the cooling circuit with the narrowest gap. Distance between cooling paths in the plasma side plates is required about 20 mm, but a pipe whose outer diameter is 8 to 10 mm cannot be bent at such a short distance and the plasma side plates cannot be manufactured in an integrated plate by the concept shown in Fig. 5. On the other hand, direct manufacturing of cooling circuit into a single plate by milling or drilling needs many welding parts for forming vacuum boundary on the plate and a high risk of vacuum leakage from welding parts. The cooling circuit in the mirror box should be formed by pipes to minimize the risk of vacuum leakage. Therefore, the outer box has a structure that consists of multiple cooling layers combined with bolt screws as shown in Fig. 6, in order to form cooling paths with about 20 mm interval by pipes with taking manufacturability into account.

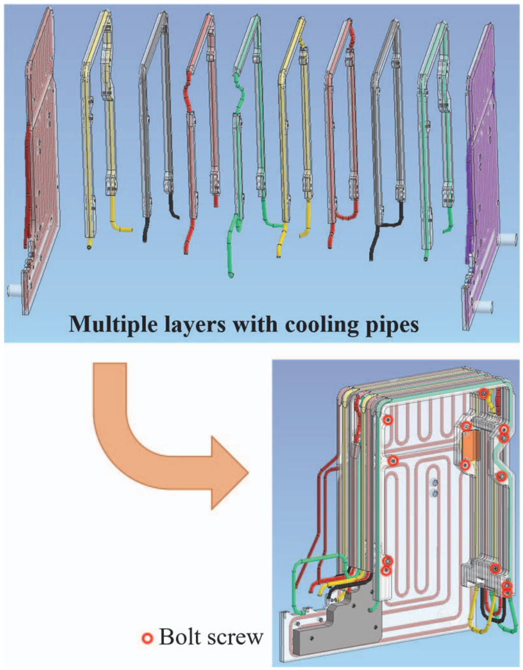

Fig. 6 Outer box structure.

The assembly procedure of the mirror box is shown in Fig. 7. The side plates are separated into lower and upper ones because the upper side plates are assembled at the final step in order to enable the access and position adjustment of the 1st to 3rd mirrors before completely closing the mirror box. The configuration of pipes is designed with taking into account the space for inserting welder.

3. Structural Analysis for Mirror Box on the Divertor Cassette

A structural integrity assessment for the mirror box shown in the previous section was carried out according to ITER load conditions, which specify some kinds of load cases such as thermal and electro-magnetic loads, and load case combinations to be taken into account. In particular, dead weight, thermal load, electro-magnetic load, acceleration from divertor, seismic load and pressure loads, as shown in Table 1, should be taken into account as representative load cases. As a first step, each single load case was analyzed in order to investigate significant loads and design drivers for the mechanical design of the mirror box. Table 1 summarizes the maximum stress value obtained due to each single load case. These results indicate that the thermal load during plasma operation and the electro-magnetic load during a plasma disruption event (VDE: Vertical Displacement Event) are significant loads for the mirror box. The analysis results for the both loads are described below.

Analysis conditions for the thermal load during plasma operation are shown in Table 2. Nuclear heating and radiative plasma heating are considered as thermal loads. Nuclear heating values are 2 MW/m^3 applied

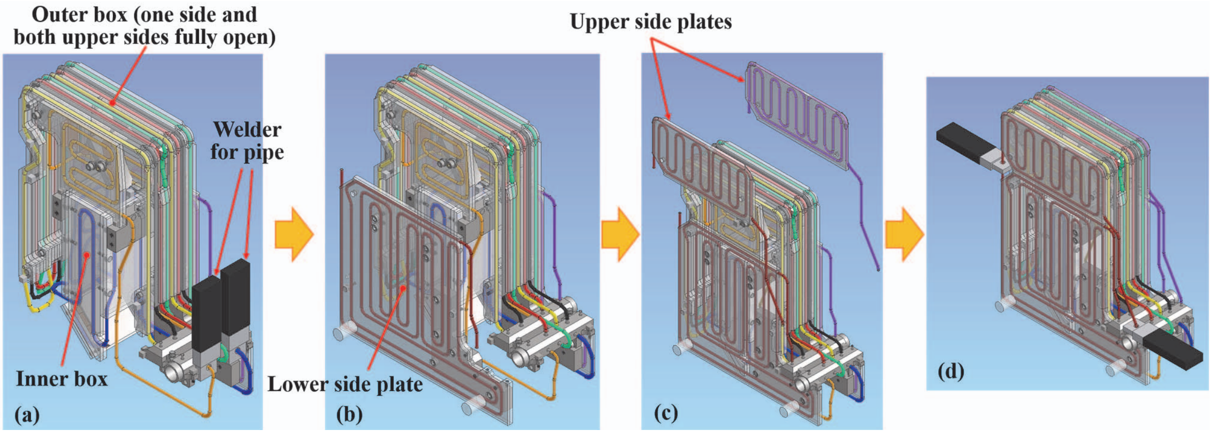

Fig. 7 Assembly procedure of the mirror box; (a) Inner box is attached inside outer box, (b) Lower side plate is attached, (c) Both upper side plates are attached after final adjustment and (d) Assembly completed.

Table 1 Summary of maximum stress due to each single load case.

Single load case (Abbreviation)	Maximum Von-Mises stress [MPa]
Dead weight (DW)	2
Thermal load during plasma operation (THO)	215
Electro-magnetic load during VDE (EM)	250
Acceleration from divertor during VDE (EM Acc.)	70
Seismic load during SL-1 event (SL-1)	2.6
Pressure load during plasma operation (PLO)	27
Pressure load during baking (PLB)	36

Table 2 Analysis conditions for the thermal load during plasma operation.

Analysis type	Steady state thermal / Static structural
Thermal loads	Nuclear heating: 2 MW/m^3 (for outer box), 1 MW/m^3 (for inner box) [5] Radiative plasma heating: 150 kW/m^2 (for plasma facing area, maximum) ~ 50 kW/m^2 (for lower area of outer box and 1st mirror surface, minimum) [6]
Cooling water	Temperature: 70 °C, Pressure: 4 MPa Fluid velocity: 2 m/s Heat transfer coefficient: 16,000 ~ 12,000 W/m^2/K (depending on the cooling path diameter: inner box 6.4 mm, outer box 8 mm, manifold 35 mm)
Thermal contact	Thermal conductance on the contact surfaces between the mirrors and the inner box plate [7] e.g. between 1st mirror and inner box plate: 82,655 W/m^2/K (Cu/Cu), 4,388 W/m^2/K (SS316L/Cu), 871 W/m^2/K (SS316L/SS316L)

for the outer box and 1 MW/m^3 applied for the inner box and mirrors [5]. Radiative plasma heating values are from maximum 150 kW/m^2 applied on the plasma facing area of the outer box to minimum 50 kW/m^2 applied on the lower area of the outer box and the reflecting surface of the 1st mirrors [6]. Heat transfer coefficient which depends on cooling path diameter is applied on cooling path area as a boundary condition for cooling. Thermal conductance on the contact surfaces between the mirrors and the inner box plate are also considered and the conductance values were calculated by Tachibana's formula [7]. Analysis results of the temperature and thermal stress distributions are shown in Figs. 8 and 9. The highest temperature is 321°C generated on the 3rd mirror close to 1st mirror and the highest thermal stress is 215 MPa generated on the inner box plate close to 1st and 3rd mirrors, the highest temperature area. Stresses obtained by elastic analysis must satisfy the following criteria;

$$P + Q < 3S_m,$$

where P is primary stress which means stress due to mechanical loads (seismic and electro-magnetic loads, etc.), Q is secondary stress which means thermal stress and S_m is the allowable stress specified in the RCC-MR [4]. S_m of SS316L at 150°C is 127 MPa. Regarding the high thermal load area at the upper side of the outer box close to plasma and around 1st mirrors, the primary stress due to mechanical loads other than thermal loads does not concentrate on the area and the value of P is sufficient lower than the maximum value of Q = 215 MPa. Therefore,

$$P + Q < 3S_m = 318\,\text{MPa},$$

is satisfied on the high thermal load area and the structural design of the mirror box is feasible for the thermal loads in the current design. However, a new requirement of radiative heating load due to reflected lights in the divertor area has been suggested [8, 9]. This effect needs to be investigated in the future study and fed back to the mirror box design.

The time change rate of magnetic fields in the mirror box due to the worst transient plasma disruption event in the divertor area is shown in Fig. 10. They are specified in the ITER load conditions, where *Bdot*(r), *Bdot*(t)

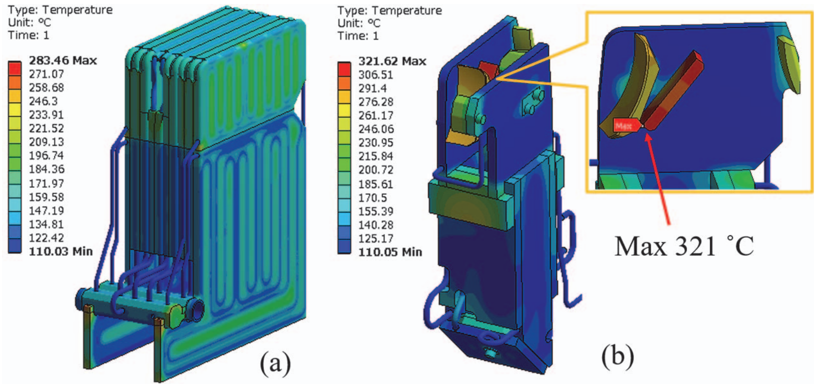

Fig. 8 Temperature distribution on (a) outer box and (b) inner box during plasma operation.

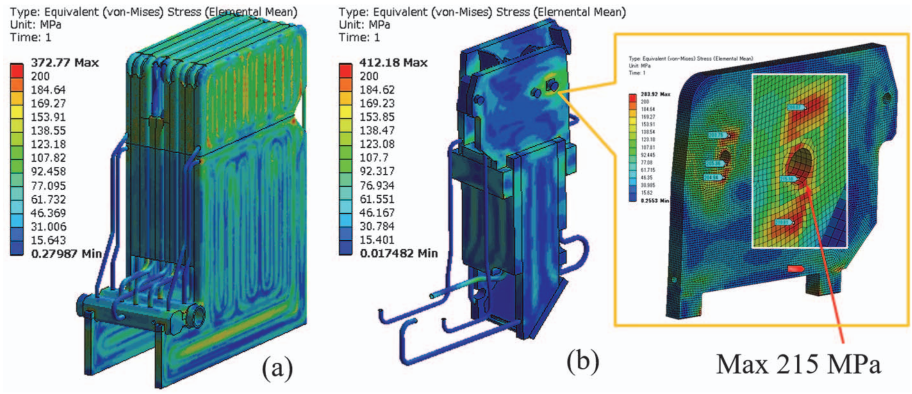

Fig. 9 Thermal stress distribution on (a) outer box and (b) inner box during plasma operation.

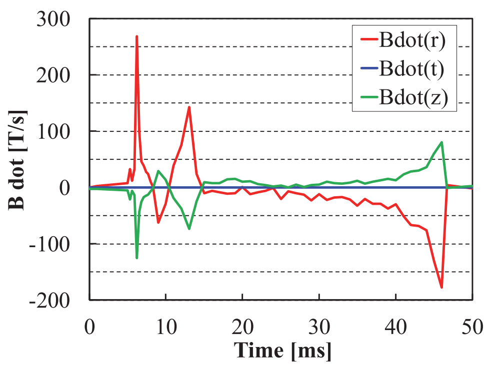

Fig. 10 Time change rate of magnetic fields in the mirror box due to a transient plasma disruption event.

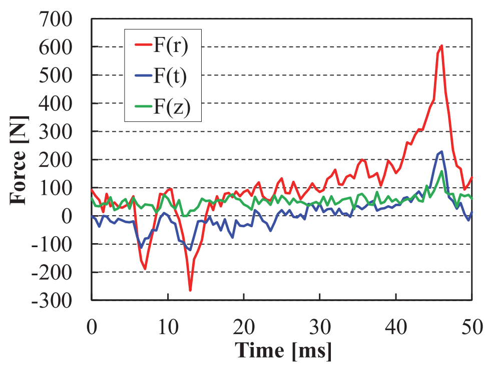

Fig. 11 Time change of electro-magnetic forces in the mirror box.

and $Bdot$(z) are the time change rates respectively in the radial, toroidal and vertical directions defined in the ITER coordinate system. The highest time change rate is 280 to 178 T/s in the radial direction. An electro-magnetic analysis was carried out by using the time change of magnetic fields. The electro-magnetic force induced for the mirror box by the magnetic field change was calculated. The results of the electro-magnetic analysis are shown in Figs. 11 and 12, time changes of electro-magnetic force and torque generated for the mirror box, where F(r), F(t) and F(z) are the time change of electro-magnetic force respectively in the radial, toroidal and vertical directions, T(r), T(t) and T(z) are the time change of electro-magnetic torque in the same manner. The highest electro-magnetic force occurs at 46 ms. The electro-magnetic force vector distribution at 46 ms is shown in Fig. 13. A structural analysis was carried out by using the electro-magnetic force distribution shown in Fig. 13 as the static load. The analysis result of stress distribution is shown in Fig. 14. The highest stress is 250 MPa generated on an inner support part, which the analysis modeling is simplified, interfacing with the diver-

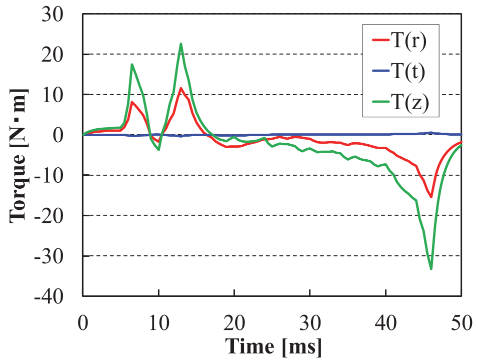

Fig. 12 Time change of electro-magnetic torques in the mirror box.

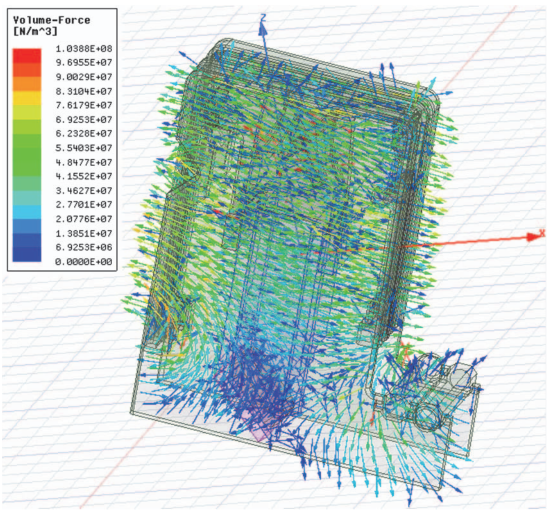

Fig. 13 Electro-magnetic force vector distribution in the mirror box.

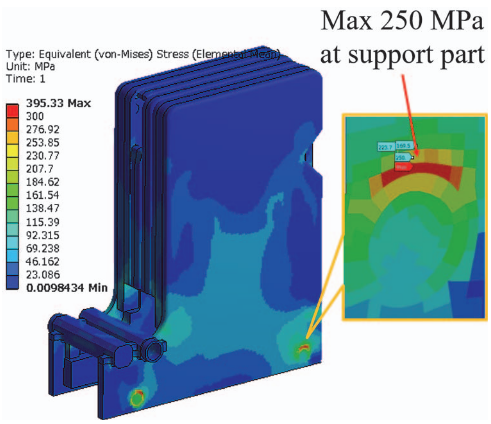

Fig. 14 Stress distribution due to electro-magnetic force in the mirror box.

tor cassette. The primary stress due to mechanical loads is prone to concentrate on the support parts.

In the ITER load conditions, specific combined load cases must be assessed for structural integrity. The analysis results indicate that the worst combined load case

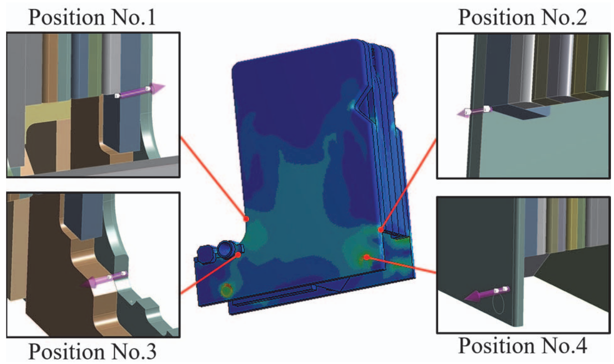

Fig. 15 Positions where the primary stress concentrates.

Table 3 Stress categorization for the worst load case, DW + PLO + SL-1 + EM + EM Acc. + THO.

Position No.	Scalar sum of stresses [MPa]		Allowable stress of SS316L [MPa]
1	P_m	63	S_m = 127
	P_L+P_B	149	1.5 S_m = 191
	P + Q	236	3 S_m = 381
2	P_m	39	S_m = 127
	P_L+P_B	178	1.5 S_m = 191
	P + Q	242	3 S_m = 381
3	P_m	125	S_m = 127
	P_L+P_B	189	1.5 S_m = 191
	P + Q	251	3 S_m = 381
4	P_m	141	S_m = 127
	P_L+P_B	340	1.5 S_m = 191
	P + Q	460	3 S_m = 381

for the mirror box is DW (dead weight) + PLO (pressure load during plasma operation) + SL-1 (Seismic load during a aSL-1 event) + EM (electro-magnetic load during a VDE) + EM Acc. (acceleration from divertor during a VDE) + THO (thermal load during plasma operation). Primary stresses due to mechanical loads at the points where the stress concentrates were categorized to obtain the membrane, local membrane and bending stresses and their stress criteria were assessed according to the RCC-MR [4]. The positions where the primary stress concentrates are shown in Fig. 15 and the categorized stresses and criteria for the worst load case at these points, where P_m is membrane stress, P_L is local membrane stress and P_B is bending stress, are summarized in Table 3. Stresses on most points satisfy the allowable ones, but the stress on the support part is higher than the allowable one. Since the stress on the support part is localized due to the simplified analysis modelling, a more detail structure of the support parts will be considered and a more detailed analysis will be carried out. Since the electro-magnetic load due to a transient plasma disruption event is significant as a mechanical load, the rigidity of the support parts will need to be enhanced. On the other hand, if a radiative heating effect due to reflected lights in the divertor area is significant, it is necessary to consider downsizing the mirror box and optics to reduce thermal and electro-magnetic loads.

4. Summary

In the central optical system for the DIM in the lower port, the optical mirrors are located under the divertor-dome to measure the inner and the outer vertical targets of the divertor cassette. A mechanical design of a box-shaped optics, mirror box, was developed so that it can withstand extremely high thermal loads in terms of establishing a sensitive optical structure. Its manufacturability was taken into account on the design. Its structural integrity assessment was carried out. Thermal and electro-magnetic loads are significant for the mirror box. The structural analysis results indicate the mirror box satisfies design criteria in the RCC-MR code, except for the inner support parts interfacing with the divertor cassette. Primary stress due to mechanical loads concentrates on the support part and electro-magnetic loads are dominant for the stress. A more detail structure of the support parts and enhanced rigidity of the support parts will be considered. On the other hand, if a radiative heating effect due to reflected lights in the divertor area is significant, it is necessary to consider downsizing the mirror box and optics to reduce thermal and electro-magnetic loads.

[1] S. Kitazawa *et al.*, Fusion Eng. Des. **101**, 209 (2015).
[2] T. Oikawa *et al.*, “Preliminary Design of Divertor Visible Spectroscopy in ITER Radiation Environment”, Rengo kouenkai, Shiga, June (2018).
[3] T. Maruyama *et al.*, Plasma Fusion Res. **11**, 2405083 (2016).
[4] RCC-MR, Design and Construction Rules for Mechanical Components of Nuclear Installations, AFCEN (2007).
[5] R. Villari *et al.*, Fusion Eng. Des. **88**, 2006 (2013).
[6] A. Encheva *et al.*, Fusion Eng. Des. **86**, 1323 (2011).
[7] F. Tachibana *et al.*, J. Jpn. Soc. Mech. Engrs. **5**, 102 (1952) (in Japanese).
[8] S. Kajita *et al.*, Plasma Phys. Control. Fusion **55**, 085020 (2013).
[9] S. Kajita *et al.*, Contrib. Plasma Phys. **56**, 837 (2016).